

ATCA search for 21 cm emission from a candidate damped Ly- α absorber at $z = 0.101$

N. Kanekar¹, J. N. Chengalur^{1,4}, R. Subrahmanyan², and P. Petitjean³

¹ National Centre for Radio Astrophysics, Post Bag 3, Ganeshkhind, Pune 411 007, India

² Australia Telescope National Facility, CSIRO, Locked bag 194, Narrabri, NSW 2390, Australia
e-mail: rsubrahm@atnf.csiro.au

³ Institut d'Astrophysique de Paris - CNRS, 98bis Boulevard Arago, 75014 Paris, France
e-mail: ppetitje@iap.fr

⁴ Visiting Scientist, NFRA, PO Bus 2, 7990 AA Dwingeloo, The Netherlands
e-mail: chengalu@ncra.tifr.res.in

Received 19 October 2000 / Accepted 1 December 2000

Abstract. We report a deep search for 21 cm emission/absorption from the $z \sim 0.101$ candidate damped Lyman- α system towards PKS 0439–433, using the Australia Telescope Compact Array (ATCA). The spectrum shows a weak absorption feature – at the 3.3σ level – which yields a lower limit of 730 K on the spin temperature of the system. No H I emission was detected: the 3σ upper limit on the H I mass of the absorber is $2.25 \cdot 10^9 M_{\odot}$, for a velocity spread of $\sim 70 \text{ km s}^{-1}$. The low H I mass and the high spin temperature seem to rule out the possibility that the absorber is a large gas-rich spiral galaxy.

Key words. cosmology: observations – galaxies: individual: PKS 0439–433 – radio lines: general

1. Introduction

Damped Lyman- α (DLA) systems are objects with such high neutral hydrogen column densities ($N_{\text{HI}} \gtrsim 10^{20} \text{ cm}^{-2}$), that their optical depth in the damping wings of the Lyman- α line is appreciable. Given a background quasar, this results in a broad absorption feature, easily detectable in even moderate resolution optical spectroscopy. DLA systems are the main repository of neutral gas at high redshift ($z \sim 3$) and have, therefore, traditionally been assumed to be the progenitors of large spiral galaxies (Wolfe 1988; Prochaska & Wolfe 1997; Prochaska & Wolfe 1998). In support of this hypothesis, the comoving mass density of neutral gas in these objects at $z \sim 3$ is comparable to the stellar mass density in bright galaxies today (Storrie-Lombardi & Wolfe 2000; Storrie-Lombardi et al. 1996; Lanzetta et al. 1991), consistent with the gas having been converted into stars in the intervening period.

At low redshifts too, DLA systems are expected to be mainly associated with spiral galaxies. Rao & Briggs (1993) used the optical luminosity function and the average H I content of a given galactic morphological type to conclude that the cross section for damped absorption at $z = 0$ is dominated by large spiral galaxies; $\sim 90\%$ of the H I at $z = 0$ resides in large spirals. An alternative

to this hybrid approach to determining the local H I mass density is to directly use the observed H I mass function. The latter, as determined by blind H I surveys is, however, currently controversial. Zwaan et al. (1997) find that the mass function is well fit by a Schechter function with a fairly flat $\alpha = -1.2$ slope at the faint end; this implies that the major contributors to the H I mass density at $z = 0$ are L^* galaxies. On the other hand, Schneider et al. (1998, see also Rosenberg et al. 2000) suggest that the space density of low mass ($M_{\text{HI}} < 10^8 M_{\odot}$) galaxies is considerably larger than that predicted by the Schechter function fit of Zwaan et al. (1997); a substantial fraction of the H I at $z = 0$ may then lie in smaller systems.

In recent times, the paradigm that damped absorption is predominantly associated with large disks has come under some scrutiny (Haehnelt et al. 1998; Ledoux et al. 1998; Vladilo 1999). Hubble Space Telescope (HST) and ground-based imaging of low and intermediate redshift damped systems (Le Brun et al. 1997; Rao & Turnshek 1998; Turnshek et al. 2000) have shown that the absorbers are associated with a wide variety of galaxy types and not predominantly with large spiral galaxies. In addition, DLA systems appear to have low metallicities (~ 0.1 solar) (Pettini et al. 1997) and do not show the α/Fe enrichment pattern seen in low metallicity halo stars of the Milky Way (Centurión et al. 2000; see, however, Lu et al. 1996). This suggests that the DLA systems have a different IMF

Send offprint requests to: N. Kanekar,
e-mail: nissim@ncra.tifr.res.in

and/or star formation history than large spirals. Finally, in cases where the background quasar is radio-loud, 21 cm absorption studies have shown that the spin temperatures of the majority of DLA objects are typically higher than those of local spirals (see Chengalur & Kanekar (2000) and references therein). High spin temperatures arise naturally in dwarfs because these systems have low metallicities and pressures and, consequently, a larger fraction of the warm phase of H I as compared to large spiral disks (Chengalur & Kanekar 2000).

It is possible, of course, that the absorbing galaxies, though faint in the optical, are nonetheless exceedingly gas-rich, and their large H I envelopes cause them to be preferentially detected in absorption surveys. At the very lowest redshifts, the latter hypothesis can be tested through deep searches for H I 21 cm emission from the absorbers. Such searches yield direct estimates of the H I mass and can thus be used to check whether or not the optically faint galaxies which give rise to DLA absorption have anomalously large H I content. We describe, in this paper, a deep search for 21 cm emission/absorption from a candidate damped absorber at $z \sim 0.101$ towards the quasar PKS 0439–433 (Petitjean et al. 1996). The observations were carried out with the Australia Telescope Compact Array (ATCA). No emission was detected, resulting in strong constraints on the H I mass of the absorber.

2. Observations and data analysis

PKS 0439–433 was observed using the 1.5 A configuration of the ATCA on a number of occasions in December 1999 and January 2000. The total on-source integration time was ~ 65 hours. A bandwidth of 8 MHz was used for the observations, divided into 1024 channels, and centred at 1290 MHz. This yielded a velocity resolution of $\sim 1.8 \text{ km s}^{-1}$ and a total velocity coverage of $\sim 1800 \text{ km s}^{-1}$. Only *XX* and *YY* polarizations were measured. The strong source PKS 0438–436 was used for amplitude/phase and bandpass calibration; this was observed every forty minutes in each observing session. 1934–638 was used as the primary flux calibrator, and observed at least once during each observing run.

The data were analyzed using the software package MIRIAD. Some baselines of the array were found to give intermittent correlator errors. Every 30-second averaged spectrum was hence inspected – separately for each baseline – to detect and reject any correlator errors as well as to reject any obvious spectral interference. Next, the routine UVLIN was used to subtract out continuum emission from discrete sources in the field. A three-dimensional data cube was then made from the residual (i.e. continuum subtracted) visibilities; spectra for further analyses were constructed using this cube. The data from the different observing sessions were shifted to the heliocentric frame before being averaged to produce the final spectrum.

While PKS 0439–433 is unresolved by the ATCA synthesized beam, the field also contains the much stronger

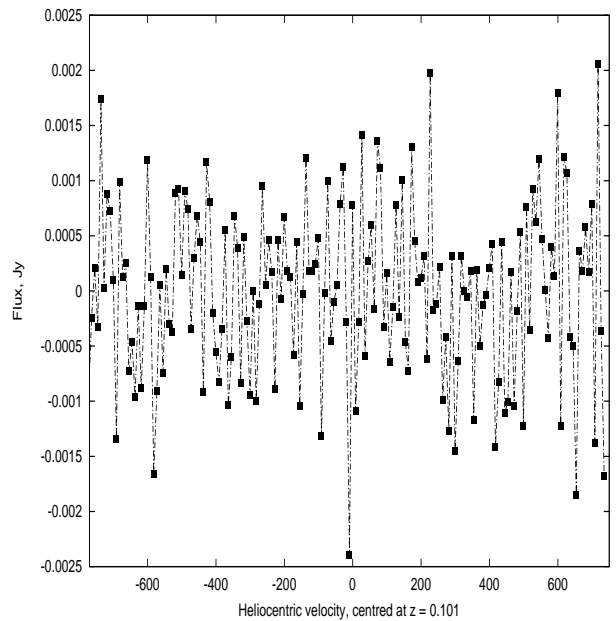


Fig. 1. ATCA 9 km s^{-1} resolution spectrum towards PKS 0439–433. The x -axis is heliocentric velocity in km s^{-1} , centred at $z = 0.101$. Weak absorption can be seen, close to $v = 0$

compact source PKS 0438–436 (flux $\sim 4.14 \text{ Jy}$, our observations), near the edge of the primary beam, as well as one more weak compact source (flux $\sim 400 \text{ mJy}$, our observations). It was thus possible that the use of UVLIN for continuum subtraction might result in spectral artefacts (Cornwell et al. 1992). We hence also tried an alternate analysis procedure to check for spectral errors that might arise due to the confusing sources in the field. This involved the use of the task UVSUB, to subtract out the individual point sources; UVLIN was then run to remove any residual continuum emission and the resulting data set was again mapped to obtain the spectral data cube. The spectra obtained from the two procedures were found to be identical within the noise for each data set.

An rms noise of 1.56 mJy was obtained per channel at the original velocity resolution of 1.8 km s^{-1} ; this is close to the theoretical sensitivity of the ATCA, for our observing parameters. Figure 1 shows the spectrum smoothed to a resolution of 9 km s^{-1} : weak absorption can be seen close to $z = 0.101$. This occurs at a heliocentric frequency of 1290.144 MHz , corresponding to a redshift of 0.10097 ± 0.00003 ; this is in good agreement with the redshift $z = 0.101$ obtained from metal lines (Petitjean et al. 1996). The rms noise on the spectrum is $\sim 0.76 \text{ mJy}$ while the feature is $\sim 2.5 \text{ mJy}$ deep (and only one channel wide), i.e. a 3.3σ result. The absorption was seen in both the *XX* and *YY* polarizations separately, although, of course, at even lower significance levels. Figure 2 shows a zoomed-in version of the spectrum at the original resolution of 1.8 km s^{-1} ; the feature of Fig. 1 can be seen to be a few channels wide here (although within the noise). We note that the narrowness of the feature makes it very unlikely

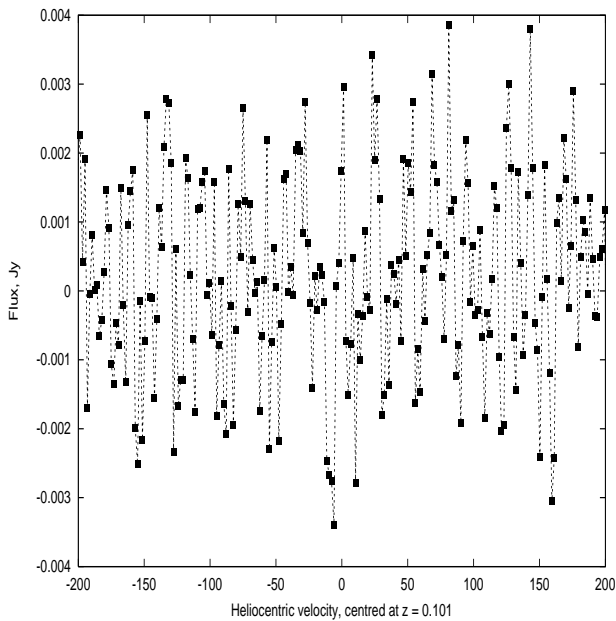


Fig. 2. Zoomed-in version of the ATCA 1.8 km s^{-1} resolution spectrum towards PKS 0439–433. The x -axis is heliocentric velocity in km s^{-1} , centred at $z = 0.101$

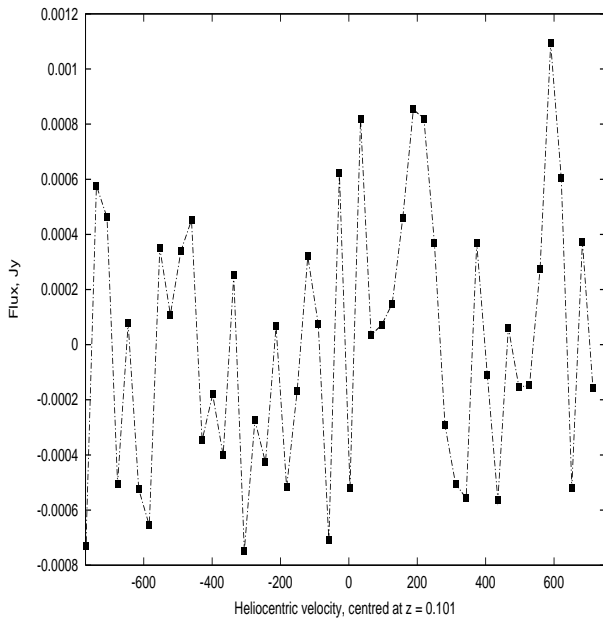


Fig. 3. ATCA 30 km s^{-1} resolution spectrum towards PKS 0439–433. The x -axis is heliocentric velocity in km s^{-1} , centred at $z = 0.101$. This spectrum was obtained after dropping antenna 6 and has a noise of 0.48 mJy

that it arises as an artefact from the continuum subtraction procedure.

The search for H I emission was done after smoothing the spectrum to a variety of velocity resolutions from 30 to 70 km s^{-1} ; no statistically significant emission was seen at any resolution. The ATCA synthesized beam (in the 1.5 A configuration), has a resolution of $\sim 15''$ on the sky, corresponding to a length scale of 18 kpc at the

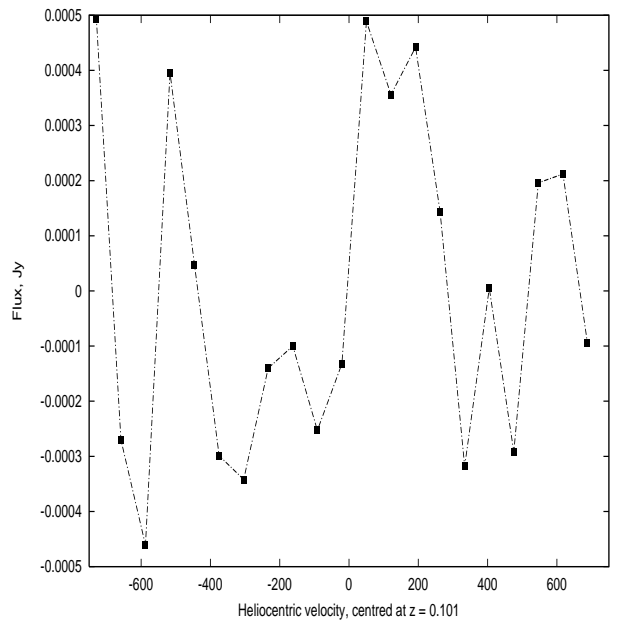


Fig. 4. ATCA 70 km s^{-1} resolution spectrum towards PKS 0439–433. The x -axis is heliocentric velocity in km s^{-1} , centred at $z = 0.101$. This spectrum was also obtained after dropping antenna 6 and has a noise of 0.29 mJy

redshift of the absorber¹. Since typical sizes of spirals tend to be larger than this ($\sim 30 - 40 \text{ kpc}$), there was a possibility that we might be resolving out some of the emission. We therefore re-analyzed the data after flagging out antenna 6, which gives rise to the long ATCA baselines: this resulted in a synthesized beam of $\sim 40''$ on the sky, corresponding to a length scale of 50 kpc at $z = 0.101$. This spectrum was also searched for emission after smoothing to a variety of velocity resolutions between 30 km s^{-1} and 70 km s^{-1} : no statistically significant emission was detected. The 30 km s^{-1} and 70 km s^{-1} resolution spectra (after dropping antenna 6) are shown respectively in Figs. 3 and 4; the rms noise levels are 0.48 mJy and 0.29 mJy . Finally, the spectrum was also smoothed to a resolution of 200 km s^{-1} to search for wide emission (note that this spectrum, which is not shown here, has only seven independent points). Again, no emission was seen; the rms noise per 200 km s^{-1} channel is 0.15 mJy .

3. Discussion

3.1. The spin temperature

For an optically thin, homogenous cloud, the 21 cm optical depth τ_{21} is related to the column density N_{HI} and the spin temperature T_s by the expression (Rohlfs 1986)

$$N_{\text{HI}} = \frac{1.823 \cdot 10^{18} T_s}{f} \int \tau_{21} dV, \quad (1)$$

where T_s is in K, N_{HI} in cm^{-2} and dV in km s^{-1} . The covering factor f can usually be estimated from VLBI

¹ An FRW cosmology with $\Omega = 1$ and $H_0 = 75 \text{ km s}^{-1} \text{ Mpc}^{-1}$ is used throughout this paper.

observations; unfortunately, no such observations exist in the literature for PKS 0439–433. The source, however, has an exceedingly flat spectrum, with flux values of 330 mJy at 1.29 GHz (our observations), 320 mJy at 2.7 GHz and 300 mJy at 5 GHz (Quiniento et al. 1988), and is thus likely to be very compact. We hence assume a covering factor of unity; this should, of course, be verified by VLBI observations. Next, the $z = 0.101$ absorber towards PKS 0439–433 is a candidate damped system, with strong Mg II, Al II, Fe II, Si II and C IV absorption lines seen in the HST spectrum (Petitjean et al. 1996). The equivalent width ratios of these low-ionization lines indicate that the system is probably damped (see also Rao & Turnshek 2000), with $N_{\text{HI}} \sim 10^{20} \text{ cm}^{-2}$ (although the Lyman- α line has itself not so far been observed for this absorber). This estimate of N_{HI} agrees well with the X-ray spectrum of PKS 0439–433 which shows absorption corresponding to $N_{\text{HI}} = 2.3 \pm 0.8 \cdot 10^{20} \text{ per cm}^2$ (Wilkes et al. 1992), with a Galactic contribution of $1.3 \pm 0.1 \cdot 10^{20} \text{ per cm}^2$ (Lockman & Savage 1995). The system is thus quite likely to be a moderate column density damped absorber. Our 9 km s^{-1} resolution ATCA spectrum has a peak optical depth $\tau_{\text{max}} \sim 0.0076$; Eq. (1) then yields a column density of $N_{\text{HI}} = 1.4 \cdot 10^{17} T_s \text{ cm}^{-2}$. Combining this with the column density of Petitjean et al. (1996) gives a spin temperature of $\sim 730 \text{ K}$. Note that this is a *lower* limit to the spin temperature, since the upper limit to the optical depth is ~ 0.0076 . If the 3.3σ feature of Fig. 1 is *not* real, it would imply that the system has an even higher spin temperature. As discussed in Chengalur & Kanekar (2000), spiral galaxies tend to have low spin temperatures ($T_s \lesssim 300 \text{ K}$); it is thus unlikely that the absorber is a large spiral galaxy.

3.2. The H I mass of the absorber

The non-detection of emission can be used to place limits on the H I mass of the $z \sim 0.101$ absorber. Of course, the peak line flux is a function of the velocity distribution in the emitting gas; for a given H I mass, a cloud with a larger velocity dispersion will result in a lower peak flux. We will, for simplicity, assume a uniform velocity distribution with a width ΔV . In this case, the H I mass of the emitting cloud is related to ΔV and the line flux S by the expression

$$M_{\text{HI}} = 2.35 \cdot 10^5 S \Delta V D_L^2, \quad (2)$$

where ΔV is in km s^{-1} , S is in Jy and M_{HI} is in solar masses. D_L is the luminosity distance of the cloud in Mpc ($D_L = 413.72 \text{ Mpc}$, for a system at $z = 0.101$).

Velocity widths in dwarf galaxies are of the order of a few tens of km s^{-1} . On the other hand, in the case of spirals, the kinematics are dominated by rotation, and the velocity spreads of H I emission profiles depend crucially on the inclination of the system to the line of sight. Face-on spirals tend to have velocity widths similar to those of dwarfs, $\Delta V \sim 20\text{--}30 \text{ km s}^{-1}$; however, disks with large inclinations can have emission spread over

a few hundred km s^{-1} . Even in the latter cases, however, velocity crowding in the tangent points results in a characteristic “double-horned” profile, where each horn is $\sim 30\text{--}40 \text{ km s}^{-1}$ wide, with a wide plateau in between. In the intermediate case, of inclination angles of the order of 45° , velocity widths of $\sim 70\text{--}100 \text{ km s}^{-1}$ are common. We will hence use two velocity widths, $\Delta V = 30 \text{ km s}^{-1}$ and $\Delta V = 70 \text{ km s}^{-1}$, to obtain limits on the H I mass of the absorber.

The 30 km s^{-1} resolution spectrum, with angular resolution $\sim 40''$ (i.e. without antenna 6), yields a 3σ upper limit of 1.44 mJy on the line flux. If we assume the emission profile has $\Delta V \sim 30 \text{ km s}^{-1}$, Eq. (2) gives $M_{\text{HI}}(3\sigma) < 1.6 \cdot 10^9 M_\odot$. The 70 km s^{-1} resolution spectrum has a 3σ upper limit of 0.87 mJy on the emission; for $\Delta V = 70 \text{ km s}^{-1}$, this gives $M_{\text{HI}}(3\sigma) < 2.25 \cdot 10^9 M_\odot$. Both the above estimates are smaller than the H I mass of the Milky Way, for which $M_{\text{HI}} \approx 5 \cdot 10^9 M_\odot$. Finally, the 200 km s^{-1} resolution spectrum also rules out the possibility that the emission is spread over a wide velocity range; this spectrum yields an upper limit of $M_{\text{HI}}(3\sigma) < 3.3 \cdot 10^9 M_\odot$, again smaller than the H I mass of the Milky Way.

Petitjean et al. (1996) identified the absorber as an $L \sim 0.45 L^*$ spiral galaxy (impact parameter $\sim 7 \text{ kpc}$), from its colours in ground based images; they also estimated an inclination angle of 51° , assuming a disk morphology. The spatial resolution of the imaging was, however, not high enough to confirm the morphology. Our observations, on the other hand, show that the H I content of the absorber is less than that of normal spirals like the Milky Way, and seem to rule out the possibility that it is a large, gas-rich spiral galaxy. It is, of course, possible that the system is an early-type, gas-poor spiral. High resolution HST imaging of the absorber is necessary to resolve this issue.

The $z \sim 0.101$ absorber towards PKS 0439–433 is the second low-redshift damped Lyman- α system which has been searched for 21 cm emission, the other being the $z = 0.0912$ absorber towards the quasar OI363 (Lane et al. 2000b). Both systems have high spin temperatures ($T_s \sim 775 \text{ K}$ for the $z = 0.0912$ system, Chengalur & Kanekar 1999; Lane et al. 2000a), far higher than those of local spirals or of damped systems which have been identified as spiral galaxies ($T_s \sim 150\text{--}200 \text{ K}$). The non-detection of emission in both cases (with fairly stringent limits on the H I mass) is consistent with the suggestion of Chengalur & Kanekar (2000) that the high T_s damped absorbers are likely to be low-mass galaxies.

Acknowledgements. It is a pleasure to thank Bob Sault for help in installing MIRIAD as well as with analysis procedures. NK thanks the ATNF for hospitality during and after the observations. The Australia Telescope is funded by the Commonwealth of Australia for operation as a National Facility managed by CSIRO. This work was partly funded by a bezoekersbeurs from NWO to JNC. JNC is grateful for the hospitality offered by NFRA for the period during which part of this work was done.

References

- Centurión, M., Bonifacio, P., Molaro, P., & Vladilo, G. 2000, *ApJ*, 536, 540
- Chengalur, J. N., & Kanekar, N. 1999, *MNRAS*, 302, L29
- Chengalur, J. N., & Kanekar, N. 2000, *MNRAS*, 318, 303
- Cornwell, T. J., Uson, J. M., & Hahaad, N. 1992, *A&A*, 258, 583
- Haehnelt, M. G., Steinmetz, M., & Rauch, M. 1998, *ApJ*, 495, 64
- Lane, W., Briggs, F. H., & Smette, A. 2000a, *ApJ*, 532, 146
- Lane, W., Briggs, F. H., Kanekar, N., & Chengalur, J. N. 2000b, in preparation
- Lanzetta, K. M., Wolfe, A. M., Turnshek, D. A., et al. 1991, *ApJS*, 77, 1
- Le Brun, V., Bergeron, J., Boissé, P., & Deharveng, J.-M. 1997, *A&A*, 321, 733
- Ledoux, C., Petitjean, P., Bergeron, J., Wampler, E. J., & Srianand, R. 1998, *A&A*, 337, 51
- Lockman, F. J., & Savage, B. D. 1995, *ApJS*, 97, 1
- Lu, L., Sargent, W. L. W., Barlow, T. A., Churchill, C. W., & Vogt, S. S. 1996, *ApJS*, 107, 475
- McDonald, P., & Miralda-Escude, J. 1999, *ApJ*, 519, 486
- Petitjean, P., Théodore, B., Smette, A., & Lespine, Y. 1996, *A&A*, 313, L25
- Pettini, M., Smith, L. J., King, D. L., & Hunstead, R. W. 1997, *ApJ*, 486, 665
- Prochaska, J. X., & Wolfe, A. M. 1997, *ApJ*, 487, 73
- Prochaska, J. X., & Wolfe, A. M. 1998, *ApJ*, 507, 113
- Quiniento, Z. M., Cersosimo, J. C., & Colomb, F. R. 1988, *A&AS*, 76, 21
- Rao, S. M., & Briggs, F. H. 1993, *ApJ*, 419, 515
- Rao, S. M., & Turnshek, D. A. 1998, *ApJ*, 500, L115
- Rao, S. M., & Turnshek, D. A. 2000, to appear in *ApJS* [[astro-ph:9909164](#)]
- Rosenberg, J. L., & Schneider, S. E. 2000, to appear in *ApJS* [[astro-ph:0004205](#)]
- Rohlfs, K. 1986, *Tools of Radio Astronomy* (Springer-Verlag, Berlin-Heidelberg)
- Schneider, S. E., Spitzak, J. G., & Rosenberg, J. L. 1998, *ApJ*, 507, L9
- Storrie-Lombardi, L. J., McMahon, R. G., & Irwin, M. J. 1996, *MNRAS*, 283, L79
- Storrie-Lombardi, L. J., & Wolfe, A. M. 2000, to appear in *ApJ* [[astro-ph:0006044](#)]
- Turnshek, D. A., Rao, S. M., Lane, W., Monier, E., & Nestor, D. 2000, to appear in *Proceedings of the Gas and Galaxy Evolution Conference*, ed. J. E. Hibbard, M. P. Rupen, & J. H. van Gorkom [[astro-ph:0009096](#)]
- Vladilo, G. 1999, in *The Evolution of Galaxies on Cosmological Time Scales*, ed. J. E. Beckman, & T. J. Mahoney, *ASP Conf. Ser.*, 187, 323
- Wilkes, B. J., Elvis, M., Fiore, F., et al. 1992, *ApJ*, 393, L1.
- Wolfe, A. M. 1988, in *QSO Absorption Lines: Probing the Universe*, ed. Blades et al. (Cambridge University Press)
- Zwaan, M. A., Briggs, F. H., Sprayberry, D., & Sorar, E. 1997, *ApJ*, 490, 173